ICONHIC2019
2nd International Conference on Natural Hazards & Infrastructure
23-26 June, 2019, Chania, Greece

Performance comparison of lead rubber bearing and friction pendulum isolation systems on a school in Kathmandu

T. Cross[1], L. Lombardi[1], F. De Luca[1], R. De Risi[1], J. Beardsley[1], M. de Podesta[1], R. Clark[1], J. Rushton[1], N. Alexander[1], A. Sextos[1]
University of Bristol[1]

ABSTRACT

Relative performances of a lead rubber bearing (LRB) and a friction pendulum isolation system (FPS), for a school in Kathmandu are assessed. As a result of the 2015 Gorkha earthquake, the feasibility of implementing seismic isolation on schools in Kathmandu is investigated. Kathmandu is situated in a lacustrine basin, which results in the amplification of longer period spectral ordinates. This was clearly observed in ground motion waveforms recorded during the 2015 event in the Kathmandu basin. A school is designed in the area of Bhaktapur (in the Kathmandu basin) in accordance with local and international regulations and practices. Two isolation systems are designed and compared (i.e., LRB and FPS). The two isolation systems are nonlinearly modelled in the structural analysis opensource software OpenSees and time-history analyses (THA) are carried out considering different ground motions. Two sets of ground motions are considered: (i) a code-conforming ground motion selection and (ii) a number of recordings from the Kathmandu Valley. Both isolation techniques reduce the seismic demand of the structure and make it compliant to international standards. The interaction between the typical long period basin amplification in the Kathmandu valley and the fundamental periods of the isolated structures is the key point of comparison, leading to quantitative comparisons on the applicability of base isolation techniques in basin contexts and near-source regions such as Kathmandu Valley.

Keywords: Seismic Isolation, Lead Rubber Bearing, Friction Pendulum System, Nepal, Kathmandu Valley

1. INTRODUCTION

Seismic isolation is a method of reducing the seismic loads on the superstructure of a building by decoupling it from the ground surface. This is achieved through an isolation system typically located at the base of the structure. The general properties of an isolation system are: (i) to resist gravity loads in both seismic and non-seismic condition; (ii) high horizontal deformability when subjected to seismic actions; (iii) good energy dissipation; (iv) to resist non-seismic horizontal loads such as wind, traffic, etc. and (v) to re-center after the seismic event (e.g., Dolce et al, 2004; Booth, 2014). Among different technologies for seismic isolation, two of them are common for buildings: Lead rubber bearing (LRB) systems and friction pendulum systems (FPS). Seismic isolation was first proposed in 1870 when Jules Touaillon was granted a patent for an isolation system whereby a series of spheres rested in concave surfaces on the foundation and the underside of the superstructure; this would allow lateral motions as well as a restoring force (Makris, 2018). Seismic isolation in its current form was developed in Wellington, New Zealand (Buckle & Mayes, 1990). Elastomeric isolation was first implemented in the 1960s and the lead core was subsequently added to increase the dampening effect of the device. In 1986, friction pendulum systems were first developed and were subsequently implemented for the first time in 1989 on a four-storey residential building in San Francisco (Naeim & Kelly, 1999). The use of seismic isolation has significantly increased over the last 40 years to include the use of isolators on

[1] Corresponding Author: T. Cross, *University of Bristol, tc14527@bristol.ac.uk*

bridges (Della Corte et al. 2013) as well as high risk facilities such as nuclear power plants (Whittaker et al, 2018).

Due to the high cost of isolation as well as transportation costs, seismic isolation is rarely implemented in developing countries. The United Nations Industrial Development Organisation (UNIDO) set out to erect a seismically isolated building in Indonesia using laminated rubber bearings to demonstrate the feasibility of seismic isolation in third world countries (United Nations Industrial Development Organisation, 1991). This project was designed to act as a stimulus for further implementation in developing countries, although has not subsequently proven to be successful.

Kathmandu Valley exhibits a high level of seismic activity due to its proximity to the Eurasian Plate and Indian Plate boundary and significant damage have been documented in the area as early as 1255 (Paudyal et al. 2012). Kathmandu Valley is a lacustrine basin whose depth can be up to 500m in some points. These deposits contain unconsolidated clay, silts, sand and gravel cause strong site effects whereby long period motions are amplified (Sakai et al, 2002). The thickness and properties of these sediments and the topography of the basin determine the resonant frequencies and subsequent site effects. Dominant resonant periods in the valley can reach up to 2s (Paudyal et al. 2012). Soft soils and basin effects are well known to amplify the ground shaking at higher periods (e.g., Rajaure et al. 2017), and the accurate quantification of amplification effects is such complex geological and geotechnical contexts can require more advanced approaches with respect to the typical site classification implemented in codes and based on the average shear-wave velocity in the upper 30m of soil at the site (V_{S30}), (e.g., EN 1998-1 2004).

In addition to the complex geological and geotechnical context, the Kathmandu Valley is also very close to the Main Himalayan Thrust (MHT); Kathmandu city is located just 11km from the MHT. This near-source location can be subjected to the potential occurrence of mega-crustal earthquakes as shown in recent seismological studies (Dal Zilio et al, 2019). Near source locations can be exposed to pulse motions such as Northridge, 1994 (M_W 6.7) and Chi-Chi, 2017 (M_W 7.6). These pulse motions exhibit high amplitude long period motions which can increase the lateral displacement of the isolators and increase the seismic demand on the superstructure (e.g., Mazza, 2018). This has raised concerns regarding resonance of seismically isolated structures and was reflected in the design requirements of the 1997 Uniform Building Codes (ICBO, 1997), subsequently reducing the feasibility of seismic isolation in certain near fault locations (Jangid & Kelly, 2001).

The study investigates the feasibility of seismic isolation in a challenging context in which the regional (i) economic conditions, (ii) geological and geotechnical context and (iii) seismological configuration are against the traditional design recommendations for this seismic protection strategy. An irregular case-study school in Bhaktapur is designed as fixed-based and as isolated using respectively LRB and FPS technology. The two isolation systems are nonlinearly modelled in OpenSees (McKenna, 2011) and subjected to a code-conforming set of ground motions and to five ground motions recorded in the Kathmandu Valley during the 2015 Gorkha earthquake (Rupakhety et al, 2017; USGS, 2016). The performances of the two isolation systems are compared focusing on the effect of site amplification due to basin effects.

2. THE CASE STUDY SCHOOL

Superstructure

The superstructure for this case study was designed to conform to typical schools in the Kathmandu region as well as complying with 2016 regulations for schools in Nepal as set out by the Nepalese ministry of education (Ministry of Education, 2016). It is located in Bhaktapur (lat. 27.68 long 85.44) at the center of the Kathmandu Valley. The school forms a “U shaped” structure with a central outdoor assembly area, as is common in Nepalese schools. This school is a higher secondary school therefore has students aged 17-18, it is designed for 900 students and some parts of it are as high as four-storey (Figure 1a).

The superstructure is a reinforced concrete moment resisting frame (RC MRF) since reinforced concrete is widely available in Kathmandu Valley relative to structural other suitable structural materials such as steel. The school sit on a thick RC slab allowing the superstructure to have constant displacement at the bottom of each column.

The RC design and isolation design is completed in adherence to Eurocodes whereas all structure loading is completed in adherence Nepalese building codes (NBC 103, 1994). For the design of the superstructure, ductility class low can be adopted for seismically isolated buildings as stated by Eurocode 8 (EN 1998-1 2004), allowing it to be designed in compliance with Eurocode 2 (EN 1992-1-2 2004). The structure is irregular in plan and in elevation, this is to mimic local architecture and to provide a central assembly area, as is common in Nepal. It has a non-structural masonry façade and has a roof formed of timber Pratt trusses which vary in length from 10 m – 20 m (not shown in Figure 1a). A 50,000L water tank is positioned on the roof of the structure as indicated by a x this allows delivery of water at a rate of 2400 L/min which allows the building to adhere to Nepalese sanitary and plumbing design requirements (NBC 208, 1994)

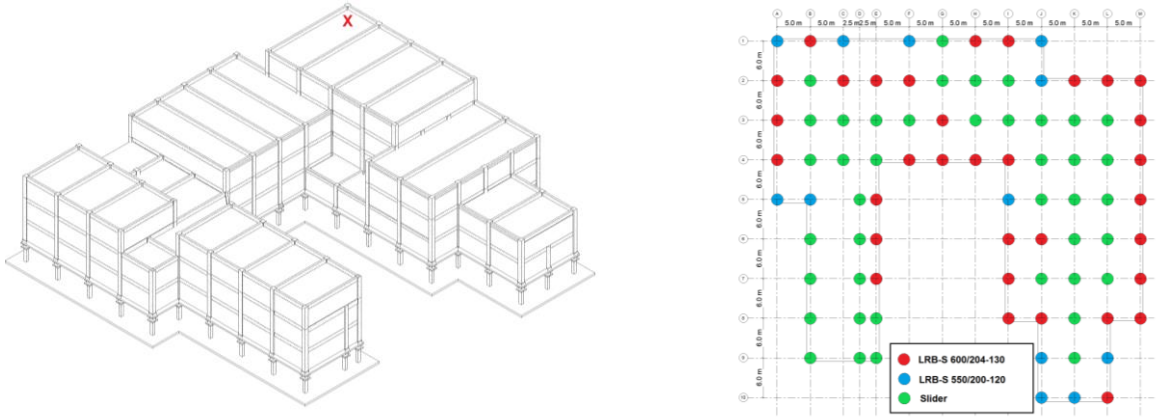

(a) (b)

Figure 1. (a) 3D view of the school with indication of the location of the water tank, (b) plan view showing isolator positions for LRB design

LRB design

The LRB design employs two different types of isolators as well as sliders (see Figure 1b). These sliders offered no lateral stiffness or dampening. The isolators must be positioned at the edge of the structure as they are to be replaced after an earthquake, of large enough magnitude to cause the lead core to yield (Govardhan & Paul, 2016). Using two different types of isolators, each with a different effective stiffness, allows the centre of stiffness to be positioned close to the centre of mass. This reduces torsion of the structure in the first two modes of vibration. Sliders are positioned under the remaining columns, which offer no lateral stiffness of dampening. The devices employed are: 33 LRB-S 600/204-130 bearings, 12 LRB-S 550/200-120 and 41 sliders as shown in Figure 1b. and Table 1.

Table 1. Summary of Isolator properties implemented in the "LeadRubberX" Element

	Symbol	**LRB-S 600/204-130**	**LRB-S 550/200-120**	**Source**
Post elastic stiffness Ratio	α	0.0577	0.0580	FIP Catalogue
Shear Modulus of Rubber	G	402.7 kN/m	415.4 kN/m	FIP Catalogue
Thickness of steel shim plates	ts	9.27 mm	10.20 mm	Calculated assuming 15 steel plates
Thickness of the rubber layers	tr	12.75 mm	12.50 mm	Calculated assuming 16 rubber layers
Number of rubber layers	n	16	16	Assumed based on example
Internal diameter	D1	130 mm	120 mm	FIP Catalogue
External Diameter	D2	600 mm	550 mm	FIP Catalogue
Mass of Bearing	mb	0.580 tonnes	0.473 tonnes	FIP Catalogue
Yield stress of the lead initially	FY10	11150 kN/m^2	11140 kN/m^2	FIP Catalogue

These bearings were implemented into the OpenSees model of the structure using the "LeadRubberX" element, as developed by Kumar et al. (2014). Table 1 defines the bearing properties for both types of isolators. Both isolators are manufactured by Fip Industriale in Italy (FIP Industriale, 2016). Several of the properties of the isolators, such as rubber bulk modulus are not published by Fip Industriale. In these cases, a value is assumed based on literature review and values provided in LRB example. All the assumptions made to define the elements in OpenSees are reported in Table 1. These properties are first implemented in a single degree of freedom (SDOF) system in OpenSees to verify the hysteretic response to horizontal motion reflect the expected one. The initial and post yield stiffness are verified and the same SDOF is also implemented in the commercial software package MIDAS Gen showing a difference in energy dissipation of less than 1% for both devices.

The seismic isolation in this structure is designed to the collapse prevention limit state defined using the Peak Ground Acceleration (PGA) value for 2475 years return period (i.e., 2% probability in 50 years). Using the probabilistic seismic hazard assessment (PSHA) developed before the 2015 Gorkha earthquake by Chaulagain et al. (2015), the design PGA is 0.65 g. After the 2015 Gorkha earthquake, a number of new PSHA studies have been published for Nepal (e.g., Stevens at al, 2018). They are based on a more refined geometry of the MHT and a different seismic source characterization and result in PGA values as high as 1g for 2475 years. These higher PGA values could result in code compliant seismic isolation not being possible using commercially available seismic isolators, due to excessive displacements; so, at this stage of the study the value of 0.65g is considered.

An elastic response spectrum is generated using as anchorage PGA a value equal to 0.65g assuming type 1 shape according to Eurocode 8 (EN 1998-1, 2004). Spectrum properties are based on ground type C as borehole data available close to the site (GEOCE Consultants Ltd. 2001) indicates a $V_{S,30}$ value of 258m/s. As the superstructure is designed in ductility class low (DCL), it is assumed to respond elastically; so, a behavior factor of 1.0 is considered.

FPS design

Unlike the LRB design, in a friction pendulum system every column is supported by an identical friction pendulum isolator. The friction pendulum isolator has an effective stiffness (K_e) calculated using equation 1, where N_{Sd} is the vertical load acting on the isolator, R is the radius of curvature, μ is the friction coefficient and d is the displacement. As each isolator has the same radius of curvature assuming the lateral displacement is equal, there should be uniform vertical displacement across the structure.

$$K_e = N_{Sd} \cdot \left(\frac{1}{R} + \frac{\mu}{d}\right) \quad (1)$$

As the effective stiffness of each isolator is directly proportional to the axial load at each column this means that the period of the isolated structure is independent of the mass of the structure and is only related to the isolator parameters. The effective stiffness being proportional to the axial load also means that the centre of mass and center of stiffness are always aligned, resulting in the first two mode shapes being translational with the third mode shape being torsional as can be seen in the mass participation masses in Table 2.

The friction pendulum isolators that are specified for this design are FIP-D M 760/800 (3700), these isolators have an effective radius of curvature of 3.7 m, a maximum vertical load capacity of 1300 kN and a friction coefficient of 5.5%. It can be seen from equation 2, employing these FPS devices, the structure has a fundamental period (T_e) equal to 3.14s. This is further verified with modal analysis results shown in the next section.

$$T_e = 2\pi \sqrt{\frac{1}{g\left(\frac{1}{R} + \frac{\mu}{d}\right)}} \quad (2)$$

The friction pendulum system was implemented into OpenSees using "singleFPBearing" elements as developed by Schellenberg (2011). The input parameter for isolators are a friction model, effective radius of curvature, and the initial elastic stiffness. The friction model used is "Coulombs law of friction" as is recommended by the FIP catalogue. The design information published by Fip Industriale (2016) implies that the isolator has a extremely high initial stiffness value (it assumes zero displacement prior to the horizontal

load exceeding the friction coefficient multiplied by the Vertical load). To accurately represent this in the OpenSees model a large initial stiffness value is used.

3. STRUCTURAL ANALYSIS

Modal properties

Modal properties were found using the effective stiffness of the isolators. The effective stiffness values are calculated assuming the isolators exhibits maximum displacement. Literature on seismic isolation shows that typically the natural period is increased to between 2s and 2.5s (Heaton et al,1995). The base isolation ratio is defined as being the ratio of the natural period of the isolated structure to the natural period of the fixed-base structure. Table 2 shows that the isolation factor for the LRB system is 2.97 and for the friction pendulum system is 4.47.
Figure 3 shows how the FPS isolation system results in regular modal shapes with respect to the fixed-base system which shows a significant torsional behavior due to the irregularity in plan of the case-study school. For sake of brevity the modes for the LRB isolated model are now shown but they are very similar to those of the FPS isolated structure (see Figure 3a - 3c).

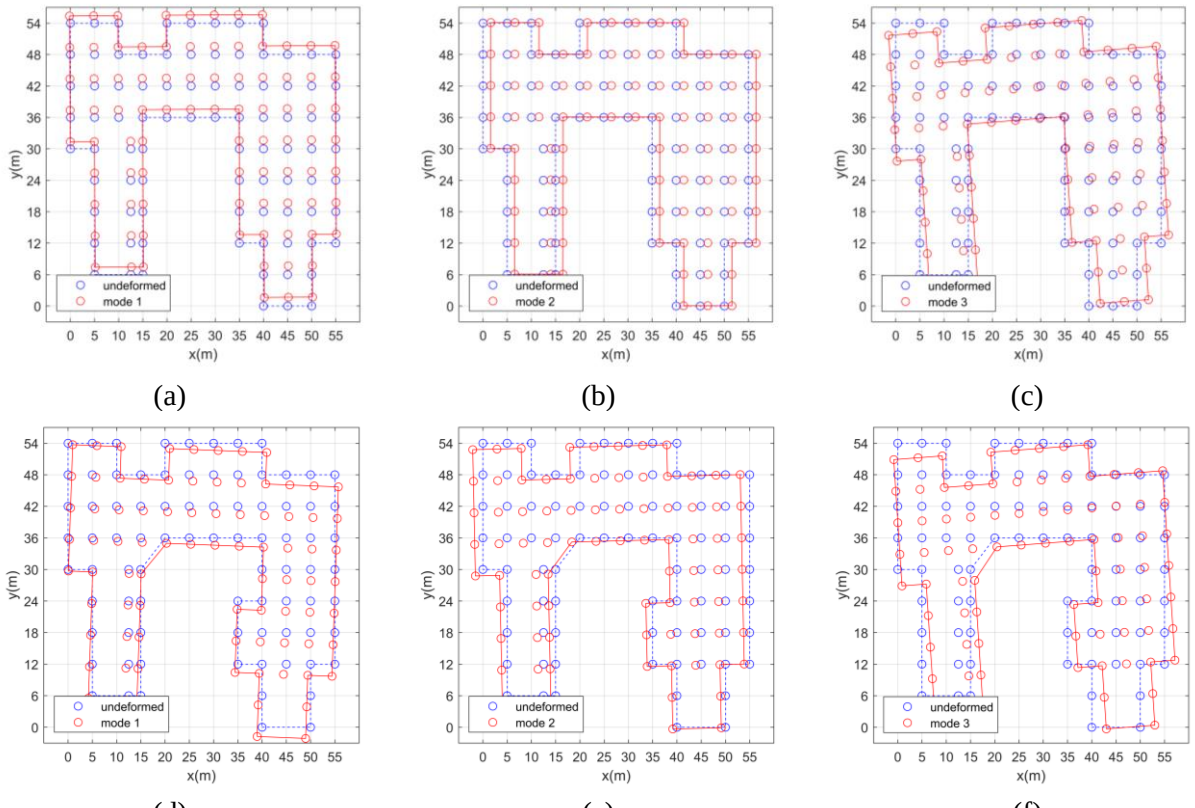

Figure 3. Mode shapes for (a) mode 1, (b) mode 2 and (c) mode 3 for the FPS isolated structures compared with (d) mode1, (e) mode 2, (f) mode 3 of the fixed-base structure.

Table 2. Modal properties of the fixed-base building and isolated with LRB and FPS.

	Fixed	**LRB**	**FPS**
Mode 1 (s)	0.70	2.08	3.14
Mode 2 (s)	0.60	2.06	3.12
Mode 3 (s)	0.54	1.86	3.11
Mode 4 (s)	0.25	0.28	0.28
Mode 5 (s)	0.25	0.24	0.24
Mode 6 (s)	0.19	0.21	0.21

Ground motion selection

Two sets of ground motions are compiled. The first set is a Eurocode 8 code compatible selection of 11 ground motions spectrum-compatible with the life-safety limit state (i.e., return period of 475 years). Between the values of $0.2T_1$ and $2.0T_1$, the arithmetic mean of the 5% damped elastic spectra of the ground motions should be no lower than the 90% of the code elastic response spectrum, where T_1 is the fundamental period of the structure. Furthermore, the mean PGA of the of the ground motions must be larger than the anchorage value of the design spectra that in this case is equal to 0.38g (Chaulagain et al. 2015). These criteria are satisfied using the Pacific Earthquake Engineering Research Center (PEER) NGA-West2 ground motion database (https://ngawest2.berkeley.edu/). Ground motions are not scaled, and each recording is from a different earthquake, exhibiting a large standard deviation within the set as expected (see Figure 4a). The recordings are summarized in Table A1 of the Appendix. The second set is formed by five couples of recordings from the 2015 Gorkha earthquake. Four of these accelerograms are from stations set up by the Faculty of Engineering, Hokkaido University, Japan (Rupakhety et al. 2017). A final ground motion record was used from the KATNP station (Kanti Path) which was managed by USGS (2016). The horizontal acceleration response spectra are shown in Figure 4b. It can observed that in the large period range the recordings in the Kathmandu Valley with the exception of KTP station, which is located on firm soil just at the boundary of the basin, show significant amplification.

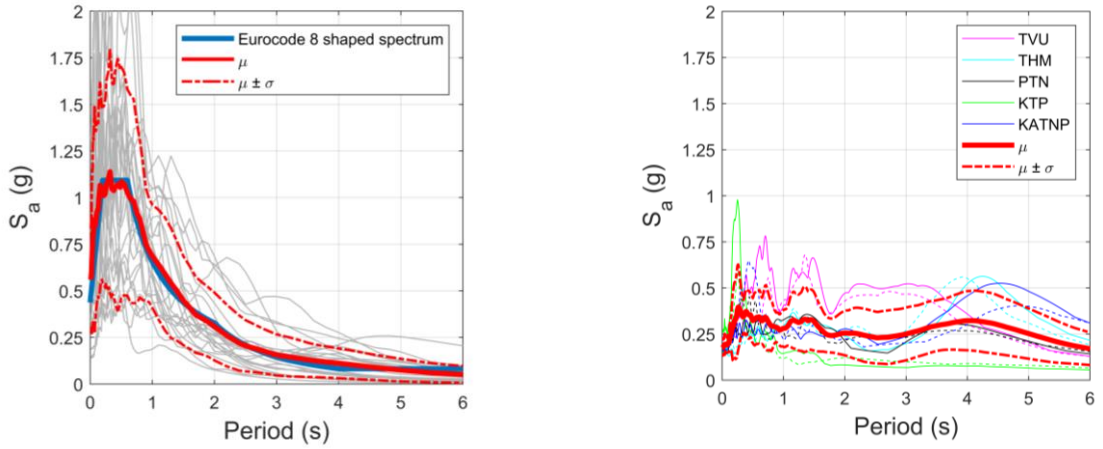

(a) (b)

Figure 4. 5% dampened spectral acceleration for (a) EC8 compliant motions (b) Gorkha 2015 motions

4. RESULTS

Inter-storey drift

Results of the time history analyses are used to find the maximum values of interstorey drift ratio (IDR) across each floor for each ground motion. This case study superstructure has a IDR limit for damage limitation state (corresponding to 95 years return period) equal to 0.5% due to the presence of brittle non-structural elements (i.e., masonry cladding). This interstorey criteria is satisfied for all ground motions for the life safety limit states as in general would be expected for isolated structures (e.g., Di Sarno et al. 2011). Figure 5 shows the mean IDR for opposing corners of the structure (i.e., A and B). This structure does not display a typical IDR profile very similar for the two corners as it would be expected. This is due to its irregularity in elevation (i.e., 3-storey in corner A and 4-storey in corner B) and due to a mass concentration in points B due to the location of the water tank (see Figure 1a).

Figure 5 shows that there is a larger seismic demand on the LRB isolated superstructure (Figure 5a and 5b) with respect to the FPS isolated structure (Figure 5c and 5d), this is clearly due to the difference in main periods as shown in Table 2. Furthermore, it can be seen in Figure 5 that the spectrum compatible PEER ground motion set (i.e., SET 1) causes a marginally larger IDR than the Gorkha set (SET 2), this is likely due to the difference in mean spectra of the two sets (see Figure 4).

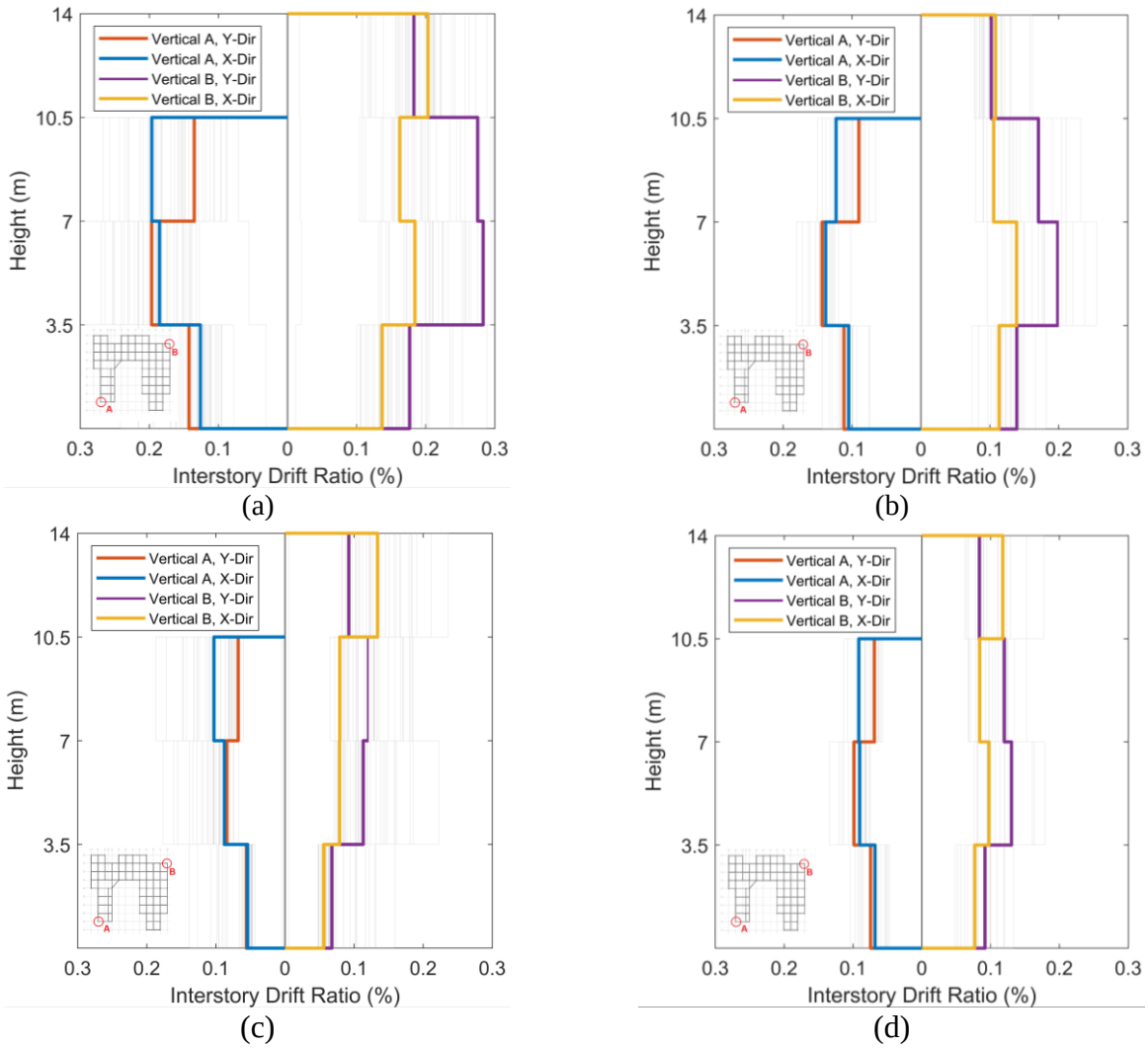

Figure 5. IDR at opposing corners of the structure LRB isolated structure with (a) PEER set (SET1), (b) Gorkha set (SET 2); FPS isolated structure with (c) PEER set (SET1), (d) Gorkha set (SET 2).

Hysteretic response

Figures 6a and 6b show the hysteretic responses of the LRB, located at the grid intersection A6 in Figure 1b, for two pairs of ground motions from SET1 and SET2, respectively. On the same plots, the idealized hysteresis of the isolator provided by the manufacturer (Fip 2016) is also shown as a dashed line. Figures 6c and 6d show the hysteretic response for the same ground motions and grid intersection indicated above, for the case of the FPS isolator. In this case, the idealized hysteresis for the FPS varies based on the vertical load applied to the isolator and therefore two idealized hysteresis are presented obtained using the maximum and minimum vertical compression axial load throughout the time history analysis.
For SET1 comparison (Figures 6a and 6c), Coyote Lake and Loma Prieta motions are chosen to represent the record-to-record variability in SET 1, since the geometric mean spectra of the two records match the confidence interval (the mean plus and minus one standard deviation) of SET1 (see dashed lines in Figure 4a). The two records considered have also very similar $V_{s,30}$ values (see Table A1).
For SET2 comparison (Figures 6b and 6d), KTP and TVU are selected to represent the highest level of spectral amplification at T_1, for both LRB and FPS isolated structures as shown in Figure 4b, due to the soil. KTP station is positioned on rock (Rajaure et al. 2017), while TVU is located on very soft soils.

The LRB response to SET1 shows a maximum level of displacement for the Loma Prieta motion as 0.111 m and the response to the Coyote Lake 0.021 m. This gives a variability factor for the confidence interval of the spectrum compatible motions as 5.3. The LRB isolated structure exhibits a displacement 0.095 m for the TVU ground motion and a displacement of 0.038 m for KTP. This gives a variability factor across SET2 as being 2.5. The FPS has a maximum displacement level of 0.406 m in response to the Loma Prieta ground motions

and a maximum level of displacement of 0.041 m in response to the Coyote Lake motions this results in a variability factor of 9.9 across the confidence interval. The FPS structure exhibits a maximum level of displacement for the TVU as 0.117 m and a maximum level of displacement in response to the KTP motion as 0.052 m. This gives a factor of variability of 2.25 across the Gorkha ground motions. For both of the isolated structures it is shown that the ground motion selection using the PEER database of unscaled records causes a larger variation in isolator displacement relative to the variation due to amplification caused by the ground type for the 2015 Gorkha earthquake.

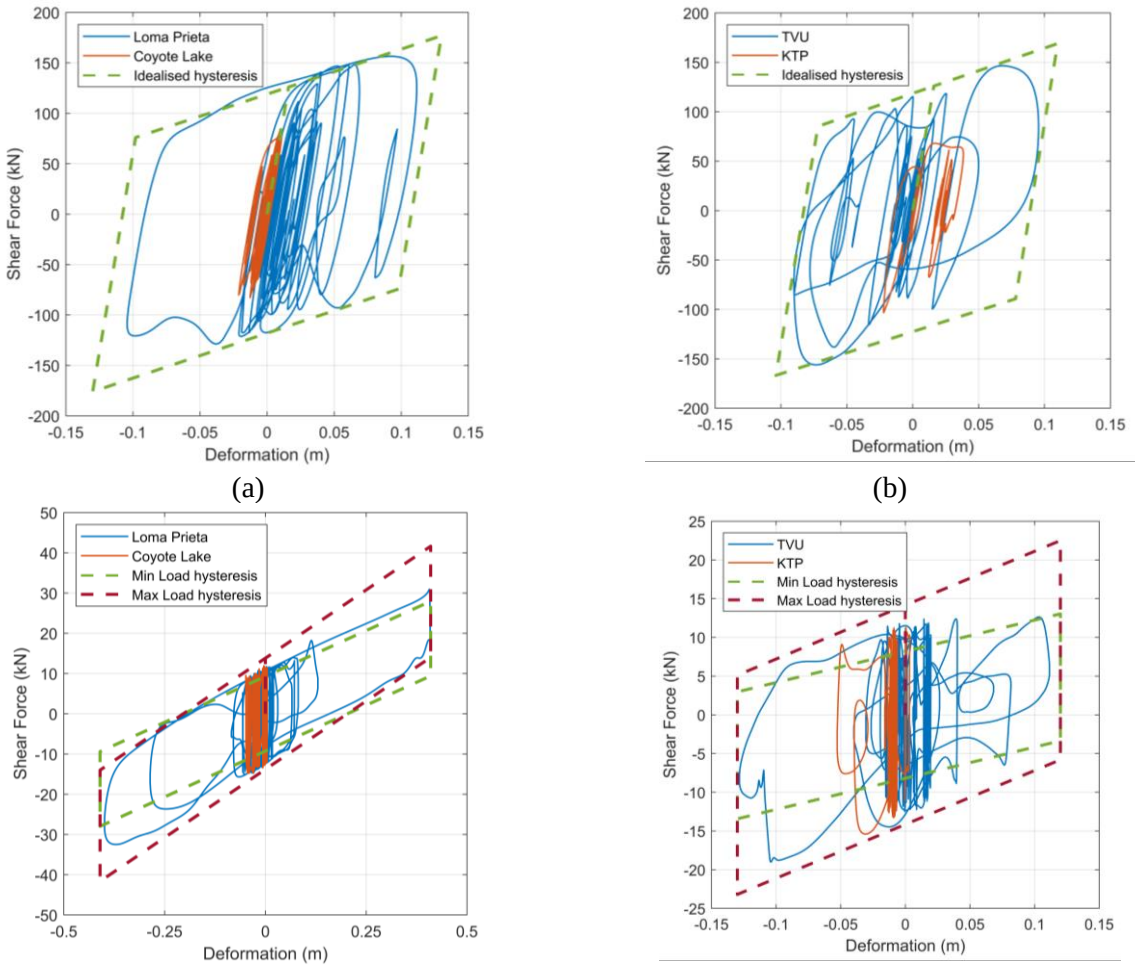

Figure 6. Hysteretic response of isolator (a) LRB-S 550/200-120 isolator with Peer motion suite, (b) LRB-S 550/200-120 isolator with Gorkha motion suite, (c) FIP-D M 760/800 (3700) isolator with Peer motion suite, (d) FIP-D M 760/800 (3700) isolator with Gorkha motion suite

5.CONCLUSION

This study presented the dynamic behavior of an irregular building isolated at the base located in Kathmandu, Nepal. Two isolation technologies have been used, isolation with rubber bearings and isolation with friction pendulum system, respectively. For the first case, the design has been carried out in order to regularize the dynamic behavior of the structure; in the second case the regular dynamic behavior is granted. With respect to the design it has been emphasized that the design can be performed only using hazard information coming from pre-Gorkha studies; when more recent hazard assessments are used, the expected design displacements of the isolation system for the collapse limit state are too high and there are no conventional devices on the market accommodating such potential displacements. Simplified non-linear dynamic analyses have been performed; the analyses are simplified since the nonlinearity is concentrated only in the isolators and the remaining part of the structure is kept elastic. The dynamic analyses have been performed considering both horizontal components of the considered seismic events. Two sets of ground motions have been used. SET1 is a set of records compatible with the EC8-type response spectrum at life-safety limit state. SET2 is the set of records available for the 2015 Gorkha earthquake.

It has been observed that both type of isolation are effective in preventing damage. Specifically, both maximum and mean inter-storey drift calculated with the two sets are well below the limitation defined for damage limitation limit state (i.e., 0.5%). Particular attention has been paid to the hysteretic behavior of the isolators. It has been observed that the maximum displacements of the isolators are larger for the friction pendulum case. Finally, from results can be inferred that the variability in the response due to the soil effect observed within the Kathmandu basin is lower than those imposed by the conventional record-to-record variability alone if the selection is done neglecting any scaling or without any control of the scatter in the ground motion set.

This is still a preliminary work and further analyses need to be carried out to confirm the obtained results. A further improvement of the study will be the modelling of the non-linearity for all the parts of the structural model.

ACKNOWLEDGEMENTS

This work was funded by the Engineering and Physical Science Research Council (EPSRC) under the project "Seismic Safety and Resilience of Schools in Nepal" SAFER (EP/P028926/1).

REFERENCES

Booth, E. D. (2014). Earthquake design practice for buildings. Third Edition, ICE Publishing, Thomas Telford, London, UK.

Buckle, I., & Mayes, R. (1990). Seismic Isolation: History, Application, and Performance. Earthquake Spectra, 6(2), 161-201.

Chaulagain, H., Rodrigues, H., Silva, V., Spacone, E., & Varum, H. (2015). Seismic risk assessment and hazard mapping in Nepal. Natural Hazards, 78(1), 583-602. doi: 10.1007/s11069-015-1734-6

Della Corte, G., De Risi, R., & Di Sarno, L. (2013). Approximate Method for Transverse Response Analysis of Partially Isolated Bridges. Journal Of Bridge Engineering, 18(11), 1121-1130. doi: 10.1061/(asce)be.1943-5592.0000473

Dhakal, Y., Kubo, H., Suzuki, W., Kunugi, T., Aoi, S., & Fujiwara, H. (2016). Analysis of strong ground motions and site effects at Kantipath, Kathmandu, from 2015 Mw 7.8 Gorkha, Nepal, earthquake and its aftershocks. Earth, Planets And Space, 68(1). doi: 10.1186/s40623-016-0432-2

Dal Zilio, L., van Dinther, Y., Gerya, T., & Avouac, J. P. (2019). Bimodal seismicity in the Himalaya controlled by fault friction and geometry. Nature communications, 10(1), 48.

Di Sarno, L., Chioccarelli, E. and Cosenza, E. (2011). Seismic response analysis of an irregular base isolated building. Bulletin of Earthquake Engineering, 9(5), pp.1673-1702.

Dolce, M., Cardone, D., Ponzo, F.C., Di Cesare, A. (2004) Design of structures with seismic isolation (in Italian). IUSS Press, Pavia.

EN 1998-1. (2004). Eurocode 8: Design of Structures for Earthquake Resistance [Ebook] (1st ed.). Brussels: BSi.

EN 1992-1-2. (2004). Eurocode 2: Design of Concrete Structures - Part 1-2 [Ebook] (1st ed.). Brussels: BSi.

FIP Industriale. (2016). Lead Rubber Bearings. Retrieved from https://www.fipindustriale.it/public/S03_LRB-eng.pdf

Fujii, R., & Sakai, H. (2002). Paleoclimatic changes during the last 2.5 myr recorded in the Kathmandu Basin, Central Nepal Himalayas. Journal Of Asian Earth Sciences, 20(3), 255-266. doi: 10.1016/s1367-9120(01)00048-7

GEOCE Consultants Ltd, (2001). Soil Drilling Log: Project: The Study on Earthquake Disaster Mitigation in Kathmandu Valley. BH-5.

Goda, K., Kiyota, T., Pokhrel, R., Chiaro, G., Katagiri, T., Sharma, K., & Wilkinson, S. (2015). The 2015 Gorkha Nepal Earthquake: Insights from Earthquake Damage Survey. Frontiers In Built Environment, 1. doi: 10.3389/fbuil.2015.00008.

Govardhan, & Paul, D. (2016). Effect of Lead in Elastomeric Bearings for Structures Located in Seismic Region. Procedia Technology, 25, 146-153. doi: 10.1016/j.protcy.2016.08.091

Heaton, T., Hall, J., Wald, D., & Halling, M. (1995). Response of High-Rise and Base-Isolated Buildings to a Hypothetical Mw 7.0 Blind Thrust Earthquake. Science, 267(5195), 206-211. doi: 10.1126/science.267.5195.206

ICBO (1997) Uniform Building Code. International Conference of Building Officials,

Whittier, C.A. Jangid, R., & Kelly, J. (2001). Base isolation for near-fault motions. Earthquake Engineering & Structural Dynamics, 30(5), 691-707. doi: 10.1002/eqe.31

Kumar, M., Whittaker, A., & Constantinou, M. (2014). An advanced numerical model of elastomeric seismic isolation bearings. Earthquake Engineering & Structural Dynamics, 43(13), 1955-1974. doi: 10.1002/eqe.2431

Makris, N. (2018). Seismic isolation: Early history. Earthquake Engineering & Structural Dynamics, https://doi.org/10.1002/eqe.3124

Mazza, F. (2018). Seismic demand of base-isolated irregular structures subjected to pulse-type earthquakes. Soil Dynamics And Earthquake Engineering, 108, 111-129. doi: 10.1016/j.soildyn.2017.11.030

McKenna, F. (2011). OpenSees: a framework for earthquake engineering simulation. Computing in Science & Engineering, 13(4), 58-66.
Ministry of Education (2016). Guidelines for Developing Type Design for School Buildings. Kathmandu, Nepal.
Naeim, F., & Kelly, J. (1999). Design of Seismic Isolated Structures: From Theory to Practice. John Wiley & Sons.
Nepalese Department of Urban Development and Building Construction. (1994). NBC 103:1994, IS 875 (part 2): 1987. Kathmandu.
Nepalese Department of Urban Development and Building Construction. (2003). Sanitary and Plumbing Design Requirements NBC 208. Kathmandu.
Paudyal, Y., Yatabe, R., Bhandary, N., & Dahal, R. (2012). A study of local amplification effect of soil layers on ground motion in the Kathmandu Valley using microtremor analysis. Earthquake Engineering And Engineering Vibration, 11(2), 257-268. doi: 10.1007/s11803-012-0115-3
Pinzón, L., Pujades, L., Diaz, S., & Alva, R. (2018). Do Directionality Effects Influence Expected Damage? A Case Study of the 2017 Central Mexico Earthquake. bulletin of the seismological society of America, 108 (5A): 2543-2555
Rajaure, S., Asimaki, D., Thompson, E. M., Hough, S., Martin, S., Ampuero, J. P., & Bijukchhen, S. (2017). Characterizing the Kathmandu Valley sediment response through strong motion recordings of the 2015 Gorkha earthquake sequence. Tectonophysics, 714, 146-157.
Rupakhety, R., Olafsson, S., & Halldorsson, B. (2017). The 2015 Mw 7.8 Gorkha Earthquake in Nepal and its aftershocks: analysis of strong ground motion. Bulletin of Earthquake Engineering, 15(7)
Sakai H, Fujii R, Kuwahara Y (2002). Changes in the depositional system of the Paleo-Kathmandu Lake caused by uplift of the Nepal Lesser Himalayas. Journal of Asian Earth Sciences, 20(3): 267-276.
Salic, R., Garevski, M., & Miltinovic, Z. (2018). Response of Lead-Rubber Bearing Isolated Structure. In The 14th World Conference on Earthquake Engineering. Beijing.
Sasaki, T., Sato, E., Okazaki, T., L.Ryan, K., A.Mahin, S., & KA.Jiwara, K. (2015). NEES/E-Defense Base-Isolation Tests: Effectiveness of Friction Pendulum and Lead-Rubber Bearings Systems. World Conference On Earthquake Engineering. Lisboa
Schellenberg, A. (2011). Single Friction Pendulum Bearing Element. Retrieved from http://opensees.berkeley.edu/wiki/index.php/Single_Friction_Pendulum_Bearing_Element
Stevens, V., Shrestha, S., & Maharjan, D. (2018). Probabilistic Seismic Hazard Assessment of Nepal. Bulletin Of The Seismological Society Of America, 108(6), 3488-3510. doi: 10.1785/0120180022
United Nations Industrial Development Organisation. (1991). Use of Natural Rubber-based Bearings for Earthquake Protection of Small Buildings. Malaysian Rubber Research & Development Board.
USGS. (2016). M 7.8 - 36km E of Khudi, Nepal Retrieved from https://earthquake.usgs.gov/earthquakes/eventpage/us20002926/executive
Whittaker, A., Sollogoub, P., & Kim, M. (2018). Seismic isolation of nuclear power plants: Past, present and future. Nuclear Engineering And Design, 338, 290-299. doi: 10.1016/j.nucengdes.2018.07.025

Appendix

This appendix provides the list of records in SET 1 and SET 2. In Table A1, recording from PEER NGA West 2 database (https://peer.berkeley.edu/research/nga-west-2) are reported providing earthquake event (Earthquake), recording station (Station), orientation of component (Orientation), year of the event (Year), average shear wave velocity in 30m (V_{s30}), Joyner-Boore distance (R_{jb}) and moment magnitude (M_W). In Table A2, station name, coordinates and location of the 5 couples of recordings from SET 2 of the 25 April 2015 Mw 7.8 Gorkha earthquake are provided.

Table A1. Code-conforming ground motion suite from PEER

Earthquake	Station	Orientation	Year	Vs30	R_{jb} (km)	M_W
Gazli, USSR	Karakyr	000, 090	1976	259.59	3.92	6.8
Coyote Lake	Gilroy Array #6	230, 320	1979	663.31	0.42	5.74
Westmorland	Westmorland Fire Sta	090, 180	1981	193.67	6.18	5.9
Loma Prieta	LGPC	090, 180	1989	594.83	0	6.93
Northridge	Newhall - Fire Sta	090, 360	1994	269.14	3.16	6.69
Kobe, Japan	Port Island (0 m)	000, 090	1995	198	3.31	6.9
Chi-Chi, Taiwan	TCU116	090, 000	1999	493.57	12.38	7.62
Duzce, Turkey	Bolu	000, 090	1999	293.57	12.02	7.14
Parkfield, CA	Parkfield - Fault Zone	090, 360	2004	246.07	8.45	6.0
L'Aquila, Italy	L'Aquila - Parking	090, 000	2009	717	0	6.3
Darfield, New Zealand	GDLC	N55W, S35W	2010	344.02	1.22	7.1

Table A2. List of the five 25 April 2015 Gorkha earthquake recordings in Kathmandu valley.

Station	Orientation	Latitude	Longitude	Location
KATNP	000, 090	27.71307	85.3161	Kanti Path
KTP	230, 320	27.68182	85.27261	Kirtipur Municipality Office
THM	090, 180	27.68072	85.3772	University Grant Commission Office, Bhaktapur
TVU	000, 090	27.68145	85.28821	Central Department of Geology
PTN	090, 360	27.68082	85.31897	Engineering College, Pulchowk